Photolytic Cage Effect. Monte Carlo Experiments

Don L. Bunker* and Barbara Slotten Jacobson

Contribution from the Department of Chemistry, University of California, Irvine, California 92664. *Received August 25, 1971*

Abstract: We have used classical trajectory analysis with Monte Carlo event selection to study the cage efficiency associated with photolysis of a diatom In a solvent of spherically symmetric molecules. For I_2 in CCl_4, our results are in adequate agreement with laboratory experience. We find that recombination efficiency is highest when recoil energy is low, solvent molecules are large, and intermolecular attractions are appreciable. The mass of the solvent molecule is not an important factor by itself. Cage recombination appears to be primarily a direct mechanical effect rather than a diffusive one. The reasons for these findings and for the failure of simple theoretical models are discussed.

In this work we have made an application of classical Monte Carlo trajectory methods. These techniques are well established, and very useful, in the study of non-Boltzmann kinetics in the gas phase. We began their extension to energetic processes in condensed phases with an investigation of nuclear recoil phenomena in inorganic phosphate crystals.[1] The research being reported here is our first venture into solution chemistry.

The problem we have chosen for this exploratory study has a long and interesting history. The suggestion that quantum yields for photolysis of solutes would be lower than for the same substances in the gas phase—a cage effect, arising from loss of energy to nearby solvent molecules—seems to have originated with Franck and Rabinowitch[2] in 1934. The simplest and most popular system for attempted demonstrations of this has been I_2 in CCl_4, which also figures in this study. A cluster of measurements[3-5] in the 1950's showed by a variety of methods that in CCl_4, I_2 photolysis in the visible range of its absorption spectrum has $\phi = {}^1/_5$–$^1/_7$ (ϕ = quantum yield, 1 for gaseous I_2, 0.08 in hexachlorobutadiene and 0.6 in hexane[3]). As was expected, escape from the solvent cage was found to be more efficient at shorter wavelengths.[5,6] Studies[3,5-7] of the effects of solvent density, viscosity, etc., have been somewhat hampered by the fact that nature does not provide a selection of liquids among which these effects can be easily separated. Only in the work of Lyon[8] in the region of the critical point has a preliminary attempt been made to isolate a single independent solvent variable (density). Nevertheless, there has been some indication, on both experimental and simple theoretical[9] grounds, that heavy solvent molecules might make a more effective cage.

The idea of a possible distinction between primary and secondary cage effects appears to have first been advanced by Noyes.[10,11] A primary cage effect is one in which the photofragments remain almost within bonding distance of one another until they lose enough energy to recombine. The secondary effect is diffusive in nature. The fragments initially separate to some distance but later find each other again. The viscosity of the solvent would affect the details of this, if the solvent is thought of as a continuous medium. In our work the solvent is composed of discrete particles, and we focus attention on the intermolecular forces rather than on the bulk viscosity. Obviously, there will be a somewhat ill-defined middle ground between these two kinds of recombination. Our convention for distinguishing them precisely will be described later.

Attempts to learn something about solvent cages by simulation with models, as we have done here, also date from early times. Rabinowitch and Wood,[9] in 1936, did a simple two-dimensional analog experiment with balls on a shaker table. With sufficient ball density, they observed groups of repetitive collisions thought to be characteristic of photochemical cage behavior. Only the ball number density was varied, not the size or mass (or of course the interball forces). Later models have concentrated on the diffusive aspects of the problem. There have been an analytical study by Noyes[12] in 1950 and a 1971 computational simulation by Walling and Lepley,[13] each involving photofragment motion on a point lattice. Both models are discussed in the later paper, and the investigators all express some misgivings about the sole adequacy of bulk properties like viscosity for the description of the molecular caging process.

This paper returns entirely to the molecular point of view. Using techniques adapted from the study of gas kinetics, we are able to simulate a photochemical recoil event in a solvent cell of minimally reasonable size in a few minutes on a moderately fast digital computer. Groups of up to 50 events for each parameter combination are feasible, and all the variables mentioned above are under direct and individual control.

Our first aim was to see whether we could observe and distinguish between the primary and secondary cage effects. All other effects of solvent parameter variation that might prove to be within our means were also slated for study. As will be seen, we have had mixed fortunes with these.

(1) D. L. Bunker and G. Van Volkenburgh, *J. Phys. Chem.*, **74**, 2193 (1970).
(2) J. Franck and E. Rabinowitch, *Trans. Faraday Soc.*, **30**, 120 (1934).
(3) F. W. Lampe and R. M. Noyes, *J. Amer. Chem. Soc.*, **76**, 2140 (1954).
(4) R. Marshall and N. Davidson, *J. Chem. Phys.*, **21**, 2086 (1953).
(5) R. L. Strong and J. E. Willard, *J. Amer. Chem. Soc.*, **79**, 2098 (1957).
(6) L. F. Meadows and R. M. Noyes, *ibid.*, **82**, 1872 (1960).
(7) D. Booth and R. M. Noyes, *ibid.*, **82**, 1868 (1960).
(8) R. K. Lyon, *ibid.*, **86**, 1907 (1964).
(9) E. Rabinowitch and W. C. Wood, *Trans. Faraday Soc.*, **32**, 1381 (1936).
(10) R. M. Noyes, *J. Chem. Phys.*, **22**, 1349 (1954).
(11) R. M. Noyes, *J. Amer. Chem. Soc.*, **77**, 2042 (1955); see also *Progr. React. Kinet.*, **1**, 129 (1961).
(12) R. M. Noyes, *J. Chem. Phys.*, **18**, 999 (1950).
(13) C. Walling and A. R. Lepley, *Int. J. Chem. Kinet.*, **3**, 97 (1971).

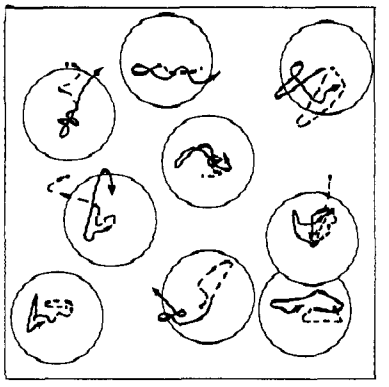

Figure 1. Projected typical motions of solvent particles during a reaction event, including the melting phase (dashed lines). One-third of the solvents, initially located in a plane, are shown. The circles have arbitrary size and represent the solvent configuration at the beginning of the reactive part of the trajectory.

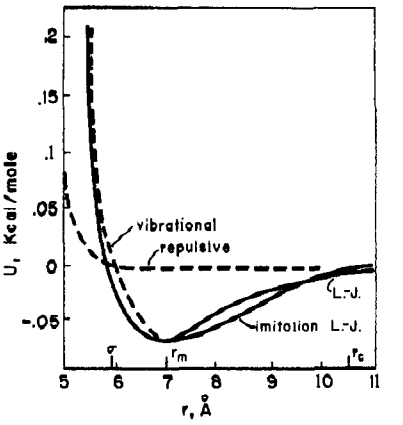

Figure 2. The four intersolvent potentials used in the work.

Methodology

The general method is as described previously.[1] New features that need discussion here are the boundary conditions on the solvent cell, the selection of initial positions and momenta, and the interaction potentials between the various particles.

The physical model we had in mind for a starting point was I_2 dissolved in CCl_4, with CCl_4 considered as a spherically symmetric, structureless particle. We treated a cubical box with a 14-Å edge, containing 26 solvent molecules. This corresponds to the real CCl_4 density. Since there are also two I's, this makes altogether (6)(28) = 168 of Hamilton's equations, solved numerically to obtain the complete details of the motion of the system.

At first we intended to impose periodic boundary conditions on the solvent particles. These, which are much used in computational studies of liquid physical properties, transpose a particle leaving the box to a diametrically opposite point and let it reenter with its vector velocity unchanged. But this turned out to introduce unwelcome correlation effects in our rather small system (*e.g.*, sometimes both I's would collide with the same solvent molecule, before and after its reentry). We found that a more satisfactory procedure is simply to make the walls of the box specularly reflect the centers of the solvent particles. We estimate that about 100 solvent molecules would need to be present before periodic boundary conditions would be the method of choice.

Initially, the I_2 is oriented along a body diagonal of the cube. Random, one at a time insertion of solvent molecules is too time consuming to be practical, so instead we start with a solid solvent and "melt" it. An orderly array of solvent molecules is set in motion, with each molecule having the same magnitude of velocity vector, but with random vector orientations. The magnitude corresponds to the average thermal energy at room temperature. After a time it is found that solvent positions have become randomized and that the corresponding momentum distribution has attained constant shape. At this point the event proper begins. The I's are propelled apart with prescribed energy, and the subsequent motion is followed until one of them escapes the box or until one of the other end conditions (described below) is recognized. Figure 1 shows typical solvent motions during the entire event.

We used several interaction potentials in this work. I–I always interacted according to the conventional Morse function. For I–CCl_4, we ordinarily used the Lennard-Jones potential

$$U = 4\epsilon[(\sigma/r)^{12} - (\sigma/r)^6] \quad (1)$$

with $\sigma = 4.968$ Å and $\epsilon = 274k$ (k = Boltzmann's constant). These values are obtained if I is equated with Xe and the usual averaging methods (arithmetic for σ and geometric for ϵ) are employed.[14] For the very numerous inter-CCl_4 interactions, the Lennard-Jones potential was much too costly; we had to avoid routinely evaluating its derivatives. We approximated it with a piecewise function with continuous first derivatives, constructed as follows. The Lennard-Jones function is used from $r = 0$ to $r = r_m$ (the minimum point of eq 1). From r_m to a cutoff point r_c, the potential is

$$U = \alpha + \beta r + \gamma r^2 + \delta r^3 \quad (2)$$

Requiring that U be continuous at r_m and that first derivatives vanish at r_m and r_c leads to

$$\alpha = \epsilon r_c^2(3r_m - r_c)/(r_c - r_m)^3 \quad (3)$$

$$\beta = -6\epsilon r_m r_c/(r_c - r_m)^3 \quad (4)$$

$$\gamma = 3\epsilon(r_m + r_c)/(r_c - r_m)^3 \quad (5)$$

$$\delta = -2\epsilon/(r_c - r_m)^3 \quad (6)$$

The exact and imitation Lennard-Jones potentials are compared in Figure 2 (the solid lines). The computational virtue of the imitation potential is that $r > r_c$ can be detected by simple tests, and much time is saved.

Two other potentials were introduced in the course of studying the sensitivity of the cage effect to solvent parameters. These will be described later.

Classification of Events

Besides other kinds of outcome, we found ourselves able to recognize four types of recombination event. Recombination in general was detected if the two I's were within Morse range of one another and without enough energy for dissociation.

(14) J. O. Hirschfelder, C. F. Curtis, and R. B. Bird, "Molecular Theory of Gases and Liquids," Wiley, New York, N. Y., 1954, pp 1110–1112.

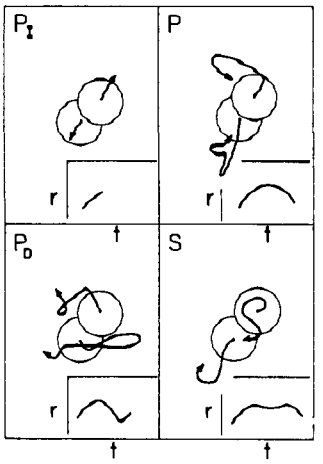

Figure 3. Projected typical I motions corresponding to the four kinds of recombination trajectory: immediate primary, P_I; primary, P; delayed primary, P_D; and secondary, S.

All the different kinds of event are tabulated, assigned symbols, and described here.

E is *escape*. One of the I's left the box.

N is *no* decision. A pretested molecule–time limit was exceeded without any other end test being met. The trajectory calculation could not be accurately continued. The I's were diffusing through the solvent at some appreciable distance from one another.

P is the uncomplicated *primary* cage effect. The I–I distance increased, attained a single maximum, and decreased again with bond formation.

P_I is a more *immediate* cage recombination in which the recombination test was met before the I–I distance reached its maximum.

P_D is a *delayed* cage effect in which the I–I distance attained its equilibrium value more than once before recombination was detected. This indicates that I remained in the cage but required more than one excursion from its initial position for I_2 to become stabilized.

S is the *secondary* cage effect. At least one shallow minimum occurred at relatively large values of the I–I distance. For the I–I distance to begin decreasing and then increase again, a solvent particle must have intervened between the I's. Nevertheless the I eventually recombined. The program was also able to detect S_D, which is similar to P_D in that more than one equilibrium value of the I–I distance occurred, but none of these events were found.

In Figure 3, the four kinds of recombination trajectory (P, P_I, P_D, S) are illustrated. All but P_I may involve fairly disorderly motion; the character of the motion does not furnish a definitive method of trajectory classification. Our restriction of the label *secondary* to events with solvent intervention is arbitrary, but it represents a clean distinction whose physical meaning is not in doubt.

Results

We present our results in the form of correlation charts. The maximum value attained by the I–I distance is plotted against the molecule time that elapsed before recombination was detected. The various kinds of outcome described above are indicated on the charts, along with an accounting of the number of E and N trajectories, if any.

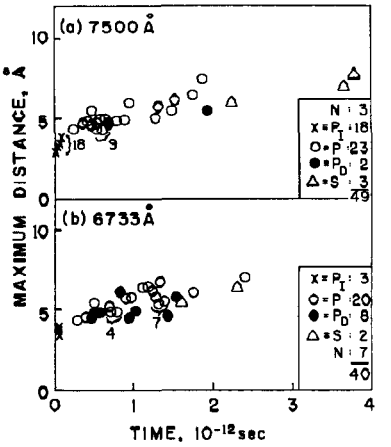

Figure 4. Results for photolysis of I_2 in CCl_4 at 7500 and 6733 Å.

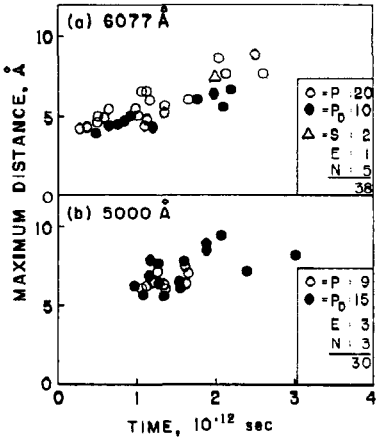

Figure 5. Results for photolysis at 6077 and 5000 Å. This is a continuation of Figure 4.

The Effect of Recoil Energy. In Figures 4 and 5 the results are shown for four I–I recoil energies. The highest, about 20 kcal/mol, corresponds to the largest value possible in the laboratory for dissociation into electronic ground states of I atoms—photolysis at about 5000 Å. The others are roughly 11 (6077), 7 (6733), and 2.5 kcal/mol (7500 Å).

It is clear that the primary cage is smallest (6 Å) at 7500 Å and largest (7.5 Å) at 5000 Å. The cage is well within the solvent box and wall effects could not have been very appreciable on the time scale of the calculations. The number of collisions in the cage required for stabilization is certainly increasing as wavelength drops, and P_I events are absent at high recoil energy. Still more interesting is the disappearance of the secondary effect at high energy. Presumably, this is because of high residual velocity and persistence of direction of motion of the high energy fragments. The three secondary events at the lowest energy appear to be a lower limit, since two of them were very long-lived, but counting the three N as probable S would still not raise the secondary effect to predominance. Although it is a statistically noisy number, the three E + three N results in 30 tries seem adequately consistent with the laboratory data.[3-5]

Since the cost of a trajectory is proportional to its length, it should be easy to see why we preferred to standardize on the 7500-Å results rather than the 5000-Å

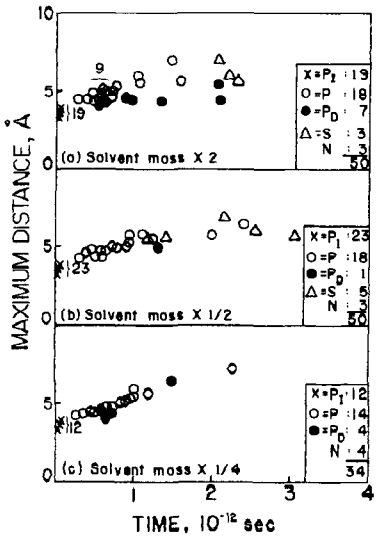

Figure 6. Results at 7500 Å when mass of solvent particle is varied. Compare Figure 4a.

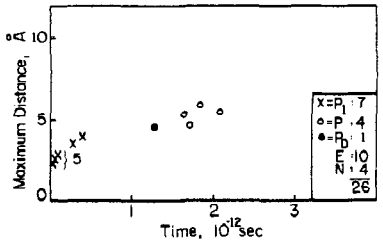

Figure 7. Results at 7500 Å with I diameters × ½. Compare Figure 4a.

ones, for comparison with further calculations. For the sake of learning something about the effects of solvent parameters, we next both tampered with the properties of CCl_4 and abandoned spectrophotometric realism for I_2.

Solvent Mass. Contrary to expectations, the effect of changing only the mass of the solvent molecule is very slight. An eightfold range of variation is shown in Figure 6, along with Figure 4a, which should be interpolated between Figures 6a and 6b. The correlation between lifetime and maximum separation is certainly smoothest at the lowest solvent mass, and the absence of secondary effects in the same data (Figure 6c) may or may not be significant. All other differences are definitely within the noise level of the computational experiments.

Molecule Size. On the other hand, the effect of changing the relative sizes of I and CCl_4 is rather striking. In Figure 7 we have shrunk I_2 by a factor of 2, leaving CCl_4 unchanged—this method having been chosen to avoid changing the box size. The caging process is dramatically less efficient. This experiment, if we had scaled the CCl_4 radius up rather than that of I down, would clearly involve a relative decrease in the mass density of the solvent. This suggests that the laboratory phenomena apparently arising from heavy solvent molecules may in reality be related to concomitant mass density (and, indirectly, size) effects. The difficulty of interpreting results for a series of real solvents with several simultaneously varying properties is well illustrated here.

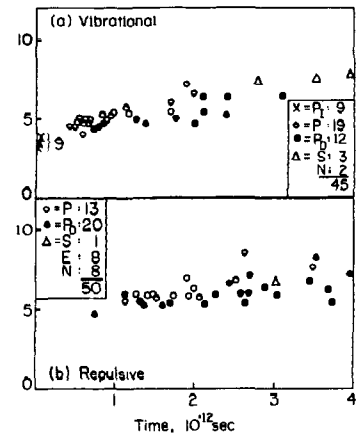

Figure 8. Results at 7500 Å for alternate potentials. Compare Figure 4a.

We would have liked to study the opposite case, a large dissociating molecule in a swarm of small solvent particles, but this would have required treating an impossibly large number of atoms.[15]

Intermolecular Potentials. For the data in Figure 8a, we replaced the Lennard-Jones repulsion from $r = 0$ to $r = r_m$ (eq 1), for both solvent–solvent and solvent–I interactions, with a quadratic function. The quadratic had zero slope at r_m and a curvature calculated from the known vibrational properties of the C–Cl bond in CCl_4. The change, which is less pronounced than we expected, is illustrated by one of the dashed lines in Figure 2. The effect of this was to change the character of the recombination events—more P_D, less P_I; compare Figure 4a—without changing the overall efficiency of the primary cage very much.

When we used the parabolic repulsion alone, with its slope set to 0 at $r = 0$ (also shown in Figure 2), we obtained Figure 8b. The character of the results is fairly strongly changed, and the cage is definitely leakier than before. Possibly this reflects a somewhat lower space-filling efficiency of the solvent; this is further discussed in the Appendix. It is difficult precisely to compare purely repulsive potentials and ones with an attractive region.

The suggestion is that gross changes in the intermolecular potentials are probably detectable at the laboratory level, but that small ones like the variation between Figures 4a and 8a are likely to show up only at the level of computational experiments.

Discussion

Because of economic limitations, we have left many things undone. We would have particularly liked to carry out the parameter comparisons with the more expensive trajectories corresponding to 20-kcal recoil energy. Also we might have studied the effects of the I–I bonding energy, and those of having photofragments with unequal masses. Much more can be done with this kind of computational experiment.

Our most striking finding is surely the relative unimportance of truly diffusive effects, involving solvent intervention, under all conditions. The low recoil energies we used should have made these effects promi-

(15) Likewise, experiments on the degree of space filling by the solvent were ruled out because we could not bring the calculation into an economical range.

nent if they are real. We concur strongly with a suggestion first made by Rabinowitch[16] and reinforced by Noyes[12] that once as many as two solvent molecules partly intervene between the photofragments, their reunion becomes highly unlikely. We would say that one intervening molecule is sufficient.

The studies of the effect of solvent size, mass, etc., that we have been able to make do not completely illuminate the situation. More work on a larger computer is needed. We do believe, however, that the mass of the solvent molecule has been overemphasized as a determinative parameter.

Our data on the effects of intermolecular forces are our least definitive, since these will surely become less important with higher recoil energy. We have established that under at least some conditions, alternative assumptions about the forces may lead to observable differences in predicted behavior.

On the whole, we conclude that a molecular description of the caging process will be preferable to one that treats the solvent as a continuous medium. On the other hand, it is fairly easy to show that a simple treatment based on the rigid-sphere radial distribution function and the character of the first collision will be inadequate. (Such a calculation is outlined in the Appendix. We have placed it there, with only enough detail to identify the arguments used, because its principal interest arises from its failure.) These simple rigid-sphere collisional considerations would suggest—not unexpectedly—that the solvent mass should be the principal parameter of interest, with the space-filling efficiency playing a secondary role. The detailed predictions match neither the laboratory evidence nor the Monte Carlo results.

The difficulty appears to be that even though cage recombination involves a single smooth maximum in the I–I separation, there are not one but several struck solvent molecules. Thus, as we have verified by inspection of the trajectories, practically all solvents have high net momentum-carrying capacity and behave as if they were made of massive molecules. The laboratory case of hexane as solvent is not necessarily an exception to this; the details are discussed in the Appendix.

To make a theory, then, we would have to consider neither the first photofragment–solvent encounter nor the bulk solvent properties, but a messy intermediate situation in which the permeability of a cluster of several particles to an energetic fragment is of interest. Until this can be accomplished and the solvent parametric dependences unscrambled, it seems likely that the kind of empirical calculation we have done will be the most attractive route to further information.

Acknowledgment. We are grateful to the National Science Foundation for supporting our work.

Appendix

The radial distribution function is $g(r)$, with r a reduced variable; for fragment (A) and solvent (S) rigid spheres of not too dissimilar size, it can be taken as

$$r = x/x_0;\quad x_0 = {}^1/_2(\sigma_A + \sigma_S) \tag{7}$$

Here x is the interparticle distance and the σ's are diameters. The probability of finding an individual particle at a reduced distance r is

$$(4\pi x_0^3/V)r^2g(r)dr \tag{8}$$

Since $g(r)$ oscillates around unity, this is normalized with respect to integration over a macroscopic container of volume V. The oscillations damp out rapidly with increasing r. The first minimum in $g(r)$ approximately bounds a first coordination sphere—best defined at high densities—and subsequent minima correspond to additional short-range order.

The average number of particles in the first layer, n_1, can be obtained by integration of (8) between $r = 1$ and r for the first $g(r)$ minimum. By geometric construction, the solid angle subtended by a solvent particle is

$$\Omega = 2\pi[1 - (1 - 1/r)^{1/2}] \tag{9}$$

and this can be multiplied by (8) and integrated over the same range to give an average value $\langle\Omega\rangle$. These integrations were done graphically from the $g(r)$ calculated and tabulated by Kirkwood, Maun, and Alder, hereafter called KMA.[17] It was found that n_1 is about 15 under conditions corresponding to Figures 4–8. Thus our simulation includes all of the first coordination shell and a portion of the second.

The quantity $n_1\langle\Omega\rangle/4\pi$, in the absence of target particle overlap, should approximate the probability of A failing to escape the first coordination shell without striking an S. From the above integrations, it is (within ±10%)

$$n_1\langle\Omega\rangle/4\pi = 2.5x_0^3\rho/M \cong (5/16)\rho(\sigma_A + \sigma_S)^3/M \tag{10}$$

In eq 10, the density ρ and the molecular weight M enter because of the V factor in (8), and the σ's are in angströms. The value of this expression is near 3 for I_2 in CCl_4, and greater than 1 in nearly all practical cases. This indicates that direct interstitial escape is usually impossible and that A always strikes one of the nearest-neighboring particles. Equation 10 could be used as a crude estimate of the probable number of S encountered. (For the data of Figure 7, this quantity is greater or less than 1 depending on how rigid-sphere diameters are estimated from Lennard-Jones parameters. It is possible that interstitial escape is a factor in these results.)

Given that an encounter is certain, we can calculate the probability that the A energy associated with motion radial with respect to the recoil site will be reduced in one collision below a stabilization threshold E_T. Let $\mathbf{v}_A$ be the initial A velocity (vector), $\mathbf{v}_S$ be the final solvent velocity, $\mathbf{v}_C$ be the component of final A velocity antiparallel to $\mathbf{v}_S$, and $\mathbf{v}_L$ be the normal component. The conservation laws are

(16) E. Rabinowitch, *Trans. Faraday Soc.*, 33, 1225 (1937).

(17) J. G. Kirkwood, E. K. Maun, and B. J. Alder, *J. Chem. Phys.*, 18, 1040 (1950); see also I. Z. Fisher, "Statistical Theory of Liquids," University of Chicago Press, Chicago, Ill., 1964, p 146. The notational difficulties may be unscrambled as follows. KMA use x where we and Fisher write r. The parameter λ^*(Fisher) = ${}^1/_2\lambda$(KMA). For the theoretical relationship between λ or λ^* and the diluteness factor v/v_0, we used the table supplied by Fisher. The average volume available to a particle is v. Fisher (and we) let $v_0 = {}^1/_6\pi\sigma_S^3$, the actual volume of a sphere, whereas KMA define v_0 as the volume attributable to one sphere in a face-centered cubic lattice. Radial distribution functions are also available for Lennard-Jones fluids (see Fisher, p 323), but their use would introduce heavy computing requirements into an otherwise simple problem.

$$m_A\mathbf{v}_A = m_A(\mathbf{v}_L + \mathbf{v}_C) + m_S\mathbf{v}_S$$

$$^1/_2 m_A v_A^2 = {}^1/_2 m_A(\mathbf{v}_L + \mathbf{v}_C)^2 + {}^1/_2 m_S v_S^2 \quad (11)$$

The projection of $\mathbf{v}_C$ on $\mathbf{v}_A$ is

$$v_R = \mathbf{v}_A \cdot (\mathbf{v}_C + \mathbf{v}_L)/v_A = \pm(2E_T/m_A)^{1/2} \quad (12)$$

where the second equality gives the bounds within which stabilization will occur. By introducing the angle θ between $\mathbf{v}_A$ and the initial A–S line of centers and integrating sin θ with limits given by the simultaneous solution of (11) and (12), we can find the probabilities for reversal, stabilization, and continued outward motion of A.

The reversal probability is

$$P_R = \frac{1 - [(1 - 1/r^2) + (m_A + m_S)(1 + E_T^{1/2}/E_A^{1/2})/2m_S)]^{1/2}}{1 - (1 - 1/r^2)^{1/2}} \quad (13)$$

in which E_A is the A recoil energy. Unless

$$2m_S/(m_A + m_S) \geq r^2(1 + E_T^{1/2}/E_A^{1/2}) \quad (14)$$

P_R is 0. The probability of stabilization, P_S, is the difference between the square root in the numerator of eq 13—or 1, if P_R is 0—and the same square root with $E_T^{1/2}$ replaced by $-E_T^{1/2}$, with the result normalized by the same denominator. It fails to exist unless

$$2m_S/(m_A + m_S) \geq r^2(1 - E_T^{1/2}/E_A^{1/2}) \quad (15)$$

An average value $\langle r \rangle$, for approximate use in these expressions, can be constructed from the KMA data by setting eq 9 equal to $\langle \Omega \rangle$. Some extrapolation from the KMA computational range may be necessary.

Using Lennard-Jones'[14] σ for σ_S, one finds that among some typical solvents the degree of space filling increases in the order CH_3OH ($\langle r \rangle$ = 1.3), C_6H_{14}, C_6H_6, CCl_4, $CHCl_3$ ($\langle r \rangle$ = 1.1). There is zero P_R for all these. The minimum E_T/E_A for stabilization is 0.58 for CH_3OH, 0.25 for C_6H_{14}, and 0.02 for CCl_4. If we say that recombination will be avoided if either photofragment escapes the cage, we need roughly P_S = 0.6 for I in hexane and P_S = 0.9 for I in CCl_4 to match the laboratory data. Both these situations require $E_T/E_A \cong {}^1/_2$, which is unrealistically high. It would require that I's retaining half their initial outward radial kinetic energy after the first collision usually recombine. For all $E_T/E_A \leq {}^1/_2$, the theory incorrectly predicts a very substantial mass effect for our Figure 6a, which should have a very much more efficient cage than in Figure 4a. Confining our attention to the immediate primary events (P_I) does not alter this, although it makes the required E_T more reasonable.

It seems inescapable that we cannot attribute stabilization to a single encounter between photofragment and solvent, and that around three successive encounters will have to be considered. For realistic (not rigid sphere) potentials, it will be preferable to view the situation as a single happening involving about four strongly interacting objects. The difficulties of making a theoretical model of this will be fairly severe.

Hydrogen Bond Interactions with Sulfur Donors

A. D. Sherry[1] and K. F. Purcell*

Contribution from the Department of Chemistry, Kansas State University, Manhattan, Kansas 66502. *Received May 26, 1971*

Abstract: Calorimetric enthalpy data are reported for the reactions of the acids, 1,1,1,3,3,3-hexafluoro-2-propanol and 2,2,2-trifluoroethanol, with six sulfur donors in CCl_4 solution and four donors in hexane solution. Frequency shift data are also reported for the same two acids reacting with eight sulfur donors. Measurement of the heats of solution of each sulfur donor in both CCl_4 and hexane allows us to estimate hexane enthalpies for the two donors whose enthalpies could not be measured directly in hexane. A comparison of oxygen and sulfur donor ΔH *vs.* ΔH and $\Delta\nu$ *vs.* $\Delta\nu$ equations reveals the greater importance of van der Waals repulsions in the sulfur donor reactions. The change in relative slopes of these equations may also be related to the greater importance of covalent contributions (C_aC_b term) to hydrogen bond formation with sulfur donors. The data adhere nicely to linear enthalpy–frequency shift relations which are considerably different from those reported previously for oxygen donors. A comparison of some analogous oxygen and sulfur donor frequency shifts reveals strong P–S π bonding in a series of phosphine sulfides.

Linear enthalpy–frequency shift relationships have been reported for phenol,[2] 1,1,1,3,3,3-hexafluoro-2-propanol[3] (HFIP), 2,2,2-trifluoroethanol[4] (TFE), *tert*-butyl alcohol,[5] and pyrrole[6] with a variety of oxygen and nitrogen donors. Anomalies from this linear behavior have been reported for the enthalpies of reaction of HFIP[3] and phenol[7] with diethyl sulfide, while the spectroscopic shifts (frequency shift *vs.* chemical shift) resulting from the reaction of this donor with HFIP

(1) National Science Foundation Research Trainee, 1970–1971; abstracted in part from the Ph.D. thesis of A. D. Sherry, Kansas State University, 1971.
(2) T. D. Epley and R. S. Drago, *J. Amer. Chem. Soc.*, **89**, 5770 (1967).
(3) K. F. Purcell, J. A. Stikeleather, and S. D. Brunk, *ibid.*, **91**, 4019 (1969).
(4) A. D. Sherry and K. F. Purcell, *J. Phys. Chem.*, **74**, 3535 (1970).
(5) R. S. Drago, N. O'Brian, and G. C. Vogel, *J. Amer. Chem. Soc.*, **92**, 3925 (1970).
(6) M. S. Nozari and R. S. Drago, *ibid.*, **92**, 7086 (1970).
(7) G. C. Vogel and R. S. Drago, *ibid.*, **92**, 5347 (1970).